Article

Improvement of the secondary aluminium metallurgical quality by means of an adequate melt treatment.

Asier Baquedano [1], Andrea Niklas [1], Ana Isabel Fernández-Calvo [1], Gorka Plata [2], Jokin Lozares [2], Carlos Berlanga-Labari [3]*

[1] AZTERLAN, Basque Research and Technology Alliance (BRTA), Durango, Spain; abakedano@azterlan.es, aniklas@azterlan.es, afernandez@azterlan.es

[2] Mechanical and Manufacturing Department, Mondragon Unibertsitatea, Loramendi 4, 20500 Mondragon, Spain; gplata@mondragon.edu, jlozares@mondragon.edu

[3] Materials and Manufacturing Engineering Research Group, Engineering Department, Institute for Advanced Materials and Mathematics (INAMAT[2]), Public University of Navarre, Campus Arrosadía s/n, 31006, Pamplona, Spain; carlos.berlanga@unavarra.es

* carlos.berlanga@unavarra.es

Abstract: This work has the purpose to demonstrate that if an adequate melt treatment is applied, it is possible to obtain recycled aluminium alloy AlSi10MnMg(Fe) with as good metal cleanliness than primary AlSi10MnMg alloy. The melt quality is assessed by the thermal analysis, density index, macro- and micro-inclusions tests, of one primary and two secondary alloys, before and after the melt treatment. The melt treatment is based on deoxidation, degassing and skimming with detailed procedure described in this article. The different analysis are: Thermal analysis to compare the variables of the solidification cooling curve (Al primary temperature and its undercooling; Al-Si eutectic temperature and its recalescence); Density index is used to evaluate the hydrogen gas content in the melt; Macroinclusions level is analysed after solidifying the melt under vacuum of 5 mbar, favouring inclusion floatation to the sample surface; Microinclusion level is evaluate with porous disc filtration apparatus (similar to PoDFA).

Keywords: melt cleanliness, secondary alloy; primary alloy; density index; inclusions; AlSi10MnMg alloy

1. Introduction

The primary aluminum alloy AlSi10MnMg is the most widely used alloy for manufacturing structural components in the automotive market, such as front shock towers, door frames and rear longitudinal members. Up to 80% of the aluminum structural components made through Vacuum High Pressure Die Casting (V-HPDC) are produced using this alloy [1]. The main reasons are: the design freedom (variation of the wall thicknesses), functional integration (able to integrate different functions in the same component), cost efficiency (mass production for complex components), weight reduction potential (very thin and low density); and finally a wide range of mechanical properties are achievable aided adequate heat treatment [2].The main difference on the components cast on conventional High Pressure Die Casting (HPDC) technology and V-HPDC technology is the ductility or energy absorption capacity [3]. The ductility obtained on parts cast by V-HPDC is significantly higher compared with the conventional HPDC technology. Considering the UNE-EN-1706:2020 standard as a reference, the minimum elongation required for the AlSi9Cu3(Fe)(Zn) alloy (the most used secondary alloy in conventional HPDC process [4-6]) is 1 % in F state, whereas for a V-HPDC component cast in AlSi10MnMg a minimum

of 12 % after T7 heat treatment is determined [3-7]. The huge difference in elongation is associated to the different composition and microstructure of both alloys, the higher melt cleanliness [7-8] and the lower porosity achieved by vacuum application in V-HPDC. The primary aluminium AlSi10MnMg alloy, generally with low iron content, (lower than 0.25 wt. %) shows a globular modified Si eutectic alongside aluminium primary dendrites. Intermetallic $Al_{12}Mn_3Si_3$ phases in the eutectic area with a polygonal-globulitic shapes are also observed. In F conditions (as-cast state) Mg_2Si intermetallic phases are present in the microstructure. These Mg_2Si phases are dissolved and then finely precipitated in the aluminium matrix after applying T6 or T7 heat treatment consisted of solution treatment, quenching and artificial aging treatment [9-12]. However, the microstructure of a secondary AlSi9Cu3(Fe)(Zn) alloy with high iron content (usually between 0.7 and 1.1 wt. %), is mainly characterized by an unmodified eutectic silicon. The intermetallic iron phases have two different shapes: polygonal-polyhedral or Chinese script denominated as α-phases or π-phases (depending on its chemical composition and its reactions); and plates phases denominated β-phases (β-Al_5FeSi). These β-phases are more harmful due to their brittle shape, and they reduce significantly the mechanical properties, especially the ductility [13-17]. There are different strategies to neutralize the effect of the harmful β-phases such us the addition of Mn, Cr, V, Be or Sr in the melt to modify the β-plates phases by iron phases with a lower harmful morphology [18-24]. However, it is also necessary that the area fraction of intermetallic compounds is maintained low and thus for achieving a good ductility Fe content as maximum of 0.6-0.7 is prescribed [22,23].

An innovational secondary aluminium alloys could be used to find comparable mechanical properties to corresponding primary alloy [9, 23, 25], with a lower economical cost, energy savings and finally generating less CO_2 emission compared to primary aluminium alloy production [26]. However, the use of secondary alloys and its applications are significantly affected by the melt cleanliness [27-28]. A proper melt treatment improves the aluminium melt quality with little capital investment and without major changes to the shop floor. The deoxidation, skimming and degassing processes show a significant improvements over the untreated melt [29].

The aim of this work is to demonstrate that if an adequate melt treatment is applied it is possible to obtain recycled aluminium alloy AlSi10MnMg(Fe) with as good metal cleanliness than primary AlSi10MnMg alloy. The new secondary AlSi10MnMg(Fe) developed in a previous work with 0.6 wt. % Fe and 0.4 wt. % Mn, which demonstrated similar high mechanical properties than primary AlSi10MnMg alloy is selected for this study [9]. Thermal analysis, density index, macroinclusions and micro-inclusions levels before and after the melt treatment in both primary and the recycled AlSi10MnMg aluminium are investigated to evaluate the effect of the melt treatment in melt cleanliness in both alloys. Regarding the secondary aluminium, two tests were performed: 1) with raw material coming from a smelter plus alloying adjustments; and 2) return from different foundries plus allowing adjustments.

2. Materials and Methods

Three different alloys were melted with the following main raw materials: a) primary ASi10MnMg ingots from Rheinfelden, b) secondary ASi10MnMg(Fe) ingots from local smelter, and c) secondary returns of two different foundries.

Figure 1: The different aluminium raw materials and its format used for the experimentation: a) Primary AlSi10MnMg ingots; b) secondary AlSi10MnMg(Fe) ingots; c) returns for secondary AlSi10MnMg(Fe) preparation.

For each experiment, 40-45 kg de each alloy were melted at 725°C in an electric furnace with a capacity of 60 kg. After melting, a simple skimming was made in the surface of the melt before starting to take the different melt samples. For achieving the target composition in terms of Si, Fe, Mn, Mg and Sr for the secondary alloy as defined in Ref [9], less than 200 g of each alloying elements were added: Si and Mg as pure elements, AlFe45 alloy (45 wt. % Fe), AlMn20 (20 wt. % Mn) and AlSr10 (10 wt. % Sr). Then, several parameters were collected using Alu Q® melt quality assessment equipment plus porous filtration test:

Thermal analysis test. The cooling curve has been plotted and analysed by Thermolan®-Al software. Main thermal analysis parameters were measured: minimum temperature of the primary Aluminium ($T_{Al\ pr\ min}$), its recalescence temperature ($Recal_{Tem\ Prim}$), and minimum Al-Si eutectic temperature ($T_{eut\ min}$). The software predicts the modification rate for HPDC parts based on the model developed in Azterlan for V-HPDC AlSi10MnMg alloys.

Density index. A sample is solidified under reduced pressure of 80 mbar (RPT) and other sample is solidified under atmospheric pressure. The Density Index (*D.I.*) is calculated according to Eq (1)

$$D.I. = \frac{\rho_{atm.} - \rho_{RTP.}}{\rho_{atm}} \times 100 \quad (1)$$

where the $\rho_{atm.}$ is the density of the sample measured at atmosphere and ρ_{RTP} is the density of the sample solidified under 80 mbar.

Macroinclusion Test. The melt sample is solidified under vacuum of 5 mbar and the macroinclusions are floating on the surface of the sample. The inclusion level of the melt is classified in a range from 1 to 10, being the 1 the worst inclusion level and 10 the optimal cleanliness situation as showing in the Figure 2.

Microinclusion level. The melt was cast into a crucible of about 2 kg capacity and the aluminum went through a filter using a vacuum system at 150 mbar (similar to PodFA). The Filtered Inclusions procedure consists on casting liquid aluminum into a crucible and passing the metal through a filter using a vacuum system. Subsequently, the metal that remains unfiltered is analysed (the metal that does not pass through the filter is where all the impurities are deposited). The inclusions observed in the filter are analysed by optical and scanning electron microscopy to identify and quantify the amount of microinclusions in the melt.
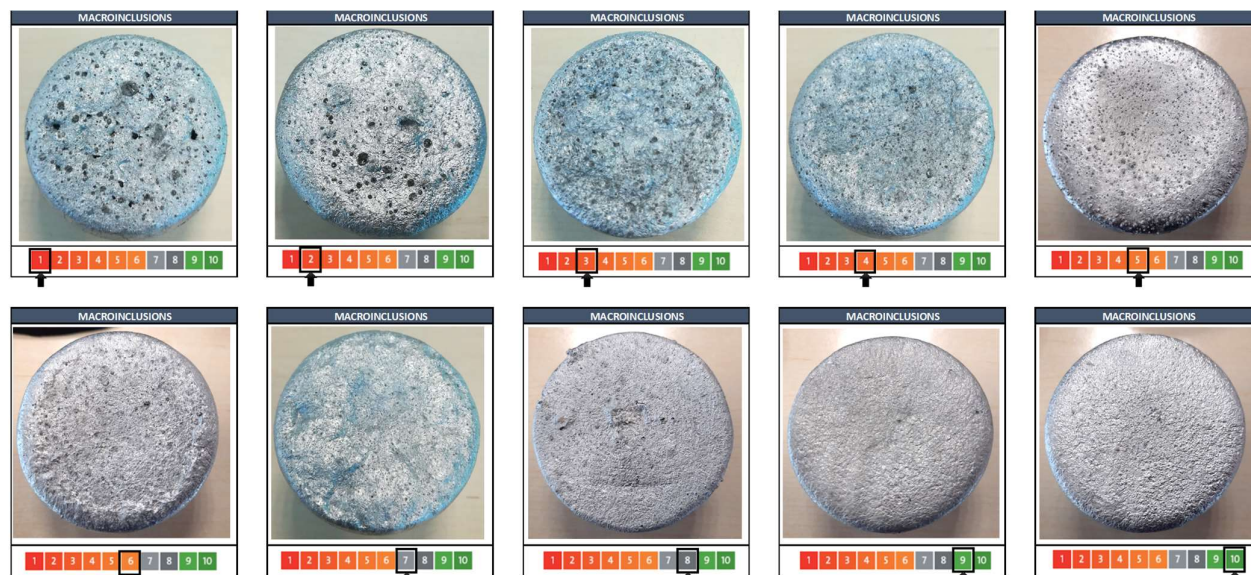
Figure 2: Macroinclusion level chart of the melt classified in a range from 1 to 10, being the 1 the worst inclusion level and 10 the optimal cleanliness situation.

After taking the samples to characterize the melt quality before the melt treatment, the melt treatment was made following the next actions: Keep the melt at 725 - 730 °C, add 100 gr of Elimoxal KF20 (a deslagging, deoxidizing and covering flux) in the surface of the melt. Make the first degassing and cleaning treatment of the melt with a rotor impeller with Ar (rotational speed: 50 rpm; Argon flux: 8 liters/min) for 10 minutes. Make the skimming and remove all slag from the melt surface. Load 100 gr of master alloy AlSr10 in cut rod format, make the second degassing and cleaning treatment of the melt with the rotor at the same rotational speed and Argon flux of previous treatment) for 15 minutes, make the skimming and remove all slag form the surface. The same melt treatment was performed for the three different alloys and samples were taken to characterize the melt quality of each alloy before and after the melt treatment.

The chemical compositions of the three alloys were analysed on spark spectrometer Spectrolab and are presented in Table 1.

Table 1. Chemical composition of the different aluminium tested in this research before and after the melt treatment (wt. %)

Reference	Status	Si	Fe	Cu	Mn	Mg	Cr	Zn	Ti	Sr
Primary alloy AlSi10MnMg	Before melt treatment	10.6	0.11	0.01	0.54	0.29	0.001	0.012	0.068	0.006
	After melt treatment	10.6	0.12	0.01	0.53	0.30	0.001	0.012	0.072	0.015
Secondary alloy AlSi10MnMg(Fe) from ingot	Before melt treatment	9.67	0.62	0.03	0.42	0.35	<0.01	0.015	0.053	<0.005
	After melt treatment	9.90	0.64	0.03	0.42	0.34	<0.01	0.015	0.052	0.013
Secondary alloy AlSi10MnMg(Fe) from returns	Before melt treatment	11.0	0.62	0.04	0.45	0.51	<0.01	0.021	0.076	0.010
	After melt treatment	10.8	0.61	0.04	0.43	0.52	<0.01	0.020	0.073	0.018

3. Results and discussion

The experimental results in terms of metallurgical quality were determined by the different tests performed. The alloys used for this work had the chemical compositions shown in Table 2. The AlSi10MnMg primary alloy shown a very low content of Fe, as well as low values of the other impurities such as Cu and Zn. Both secondary alloys have similar chemical composition, very similar to secondary alloy with medium content of Mn in Ref. 10. In comparison to the primary alloy, they present higher content of Fe with moderate content of Mn and a slightly higher content of Cu and Zn. The three alloys show quite similar Sr yield when adding of the AlSr10 master alloy.

The cooling curve of the three alloys is shown in Figure 3, and the main parameters of each cooling curve are summarized in Table 2. The secondary alloy ingot from returns presents the higher minimum temperature of the primary aluminium because it has the highest Si content of the three analysed alloys. Aluminium primary recalescence varying between 1.1-1.8 ºC, which indicates a large grain size in the analysed cup. This is coherent with the absence of addition of Ti refiners. It should be noted that the solidification rate in HPDC is so high, that natural grain refinement is achieved and thus no grain refinement is recommended in this process.
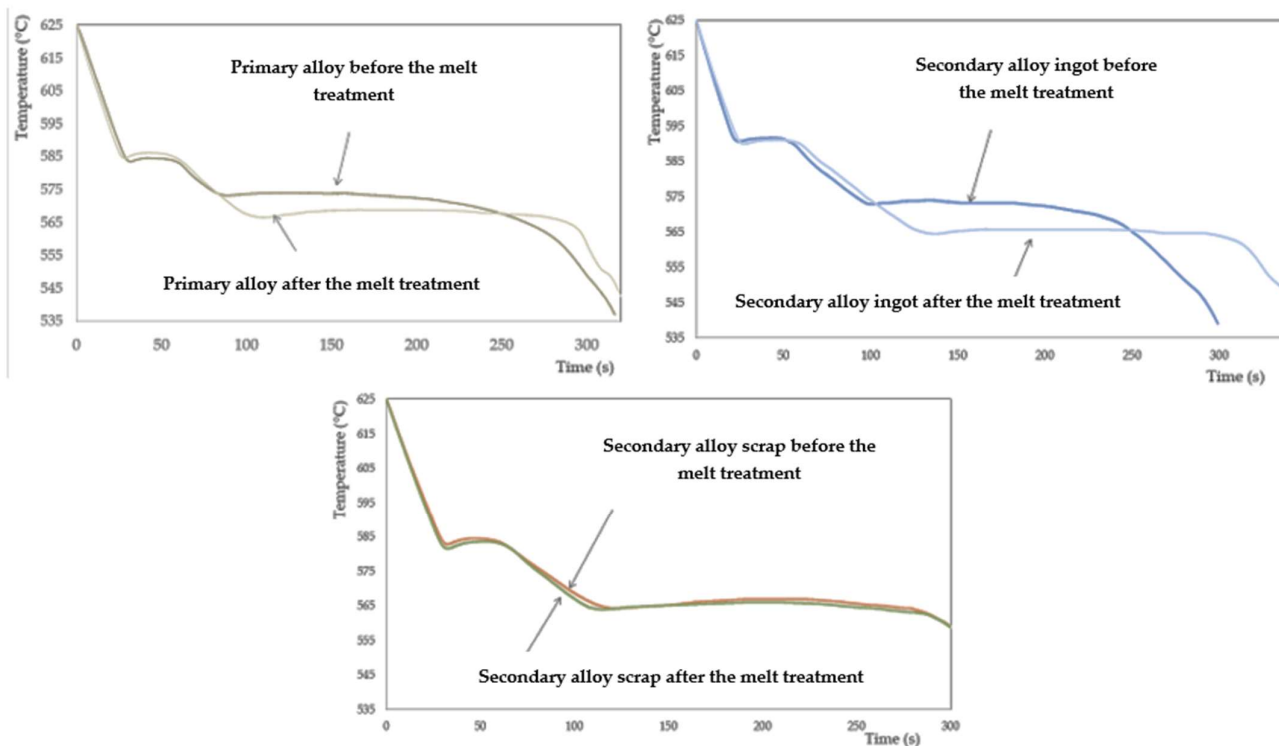

Figure 3. The cooling curve of the different alloys before and after the melt treatment.

The effect of the adding AlSr10 in the melt treatment reduces significantly the aluminium-silicon eutectic temperature in the primary alloy and in the secondary alloy from ingot, because both have a low Sr content and modification rate prediction by Thermolan®-Al shown in Table 2 is also improved by the melt treatment addition from modification rate 1-2 to 4. However, the secondary alloy from returns has the same eutectic temperature before and after the melt treatment and high modification rate prediction in both cases. The 0.010 wt. % of Sr content before the melt treatment is high enough to achieve a good modification rate in V-HPDC.

Table 2. The main cooling curve parameters and modification rate prediction of Themolan®-Al for V-HPDC AlSi10MnMg alloys.
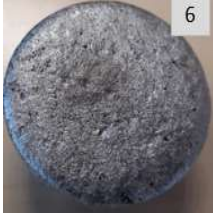
Reference	Stages	T Al prim min (°C)	Rec Al prim (°C)	T Eutec min (°C)	Modification rate prediction
Primary alloy	Before melt treatment	586.6	1.1	573.2	1-2
	After melt treatment	584.7	1.5	566.5	4
Secondary alloy ingot	Before melt treatment	590.5	1.1	573.0	1-2
	After melt treatment	590.1	1.1	564.5	4
Secondary alloy returns	Before melt treatment	582.9	1.6	564.3	4
	After melt treatment	581.7	1.8	563.9	4

The results of the density analysis obtained during the experimentation for the different aluminium alloys and the different stages (before and after the melt treatment) are shown in Figure 4. The density index of the primary aluminium alloy is significantly lower the obtained for both secondary aluminium alloys before the melt treatment. Thus, a significant lower hydrogen content in the melt is expected in this condition. However, after the melt treatment there is not significantly differences between the different alloys showing that the melt treatment has a high effectiveness in reducing the content of hydrogen in the melt below a 1 % in D.I. as was proposed by Ing. Hermann Roos et al. [30].
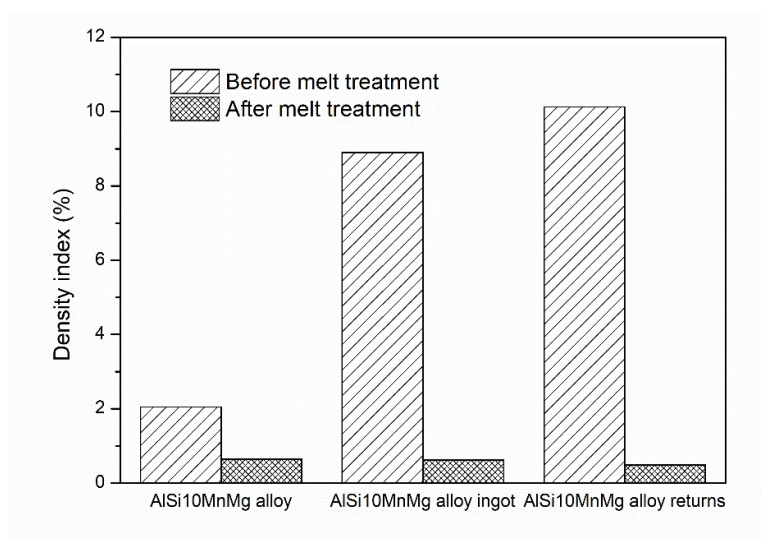
Figure 4. Values of the density index in the three alloys and stages (before and after the melt treatment).

The results of macroinclusions test analysis obtained in the different alloys and stages are shown on table 3, classified based on the naked eye comparison with the defined chart of Figure 2, as described in the experimental procedure. Before the melt treatment, the level of macroinclusions was significantly worse in the secondary alloys, being return alloy the worst one. However, after the melt treatment made to melt quality improves significantly; and the macroinclusions level in the three different alloys, achieves the same high 9 level.

Table 3. The macroinclusions level of the melt is classified following chart level of Figure 2, being the 1 the worst inclusion level and 10 the perfect situation.

Reference	Sample before melt treatment	Sample after melt treatment
Primary alloy		
Secondary alloy ingot		
Secondary alloy return		

The different samples of microinclusions tests were cut and the metallographic analysis was performed on the polished surface of the sample, more specifically on the inspection field close to the ceramic filter where the inclusions are located. Three main areas are observed in the inspection field: the ceramic filter area (1), the inclusion cake (2), and the base metal area (3) for the different alloys and its stages (before and after the melt treatment). The melt filtered is very similar in all trials, significantly higher than 500 g which is considering for the PodFA analysis the minimum required value [31].

Table 4. The filtered and no filtered melt during the different trial

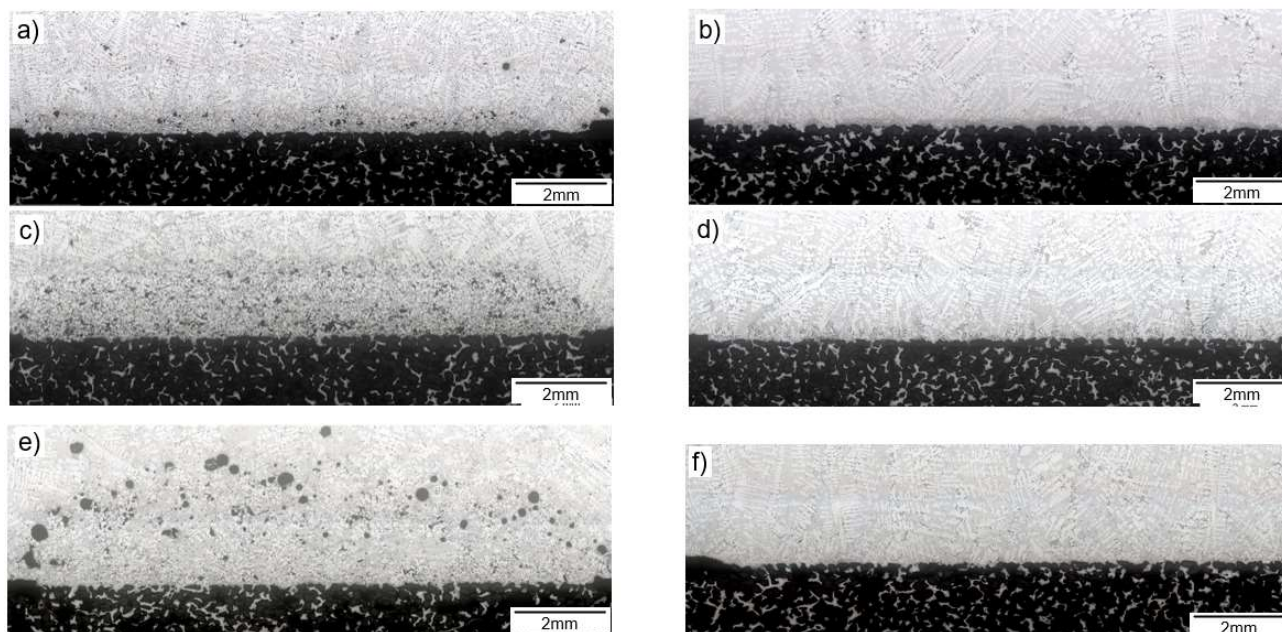| Reference	Stages	Filtered weight (g)	No filtered weight (g)	Total Weight (g)
Primary alloy	Before melt treatment	1081	942	2024
	After melt treatment	1232	660	1892
Secondary alloy ingot	Before melt treatment	1284	851	2135
	After melt treatment	1360	614	1974
Secondary alloy returns	Before melt treatment	1051	995	2046
	After melt treatment	1218	731	1949

Figure 5. The inclusions cake of the different alloys. Primary: a) before, and b) after the melt treatment: Secondary alloy ingot: c) before, and d) after the melt treatment. Secondary alloy return: e) before and f) after the melt treatment.

During the experimentation, the different filtered and no-filtered weight were measured as shown in the table 4. The thickness of the inclusion cake is shown in Figure 5 and its measurement is summarised in Table 5. Before the melt treatment the best result is in primary alloy with 472 µm, followed by the secondary alloy ingot with 1660µm (more than three times the best result) and finally secondary alloy returns with 2766 µm. However, after applying an adequate melt treatment, the thickness of the inclusion cake is reduced significantly in the three aluminium alloys, especially in the secondary aluminium alloys where the thickness is lower than 80 µm.

Table 5. Thickness of the inclusion cakes.

Reference	Before melt treatment	After melt treatment
Primary alloy	472µm	229 µm
Secondary alloy ingot	1660 µm	<80 µm
Secondary alloy scrap	2766 µm	<80 µm

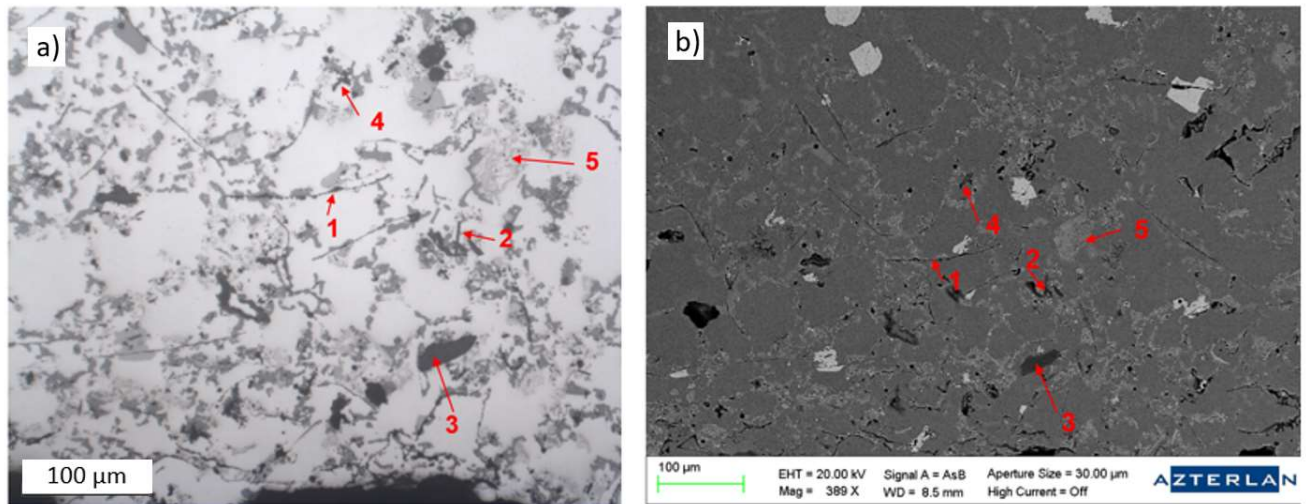The samples were analysed by optical microscopy and SEM as it is shown in the Figure 6.

Figure 6. Microinclusions identification by optical and SEM analysis of primary alloy before the melt treatment: 1) Oxides films γ-Al_2O_3, 2) Carbides Al_4C_3, 3) Large magnesium oxides and spinel $MgAl_2O_4$, 4) Oxides and others (α-Al_2O_3, CaO, SiO_2), 5) Grain refinement particles TiB_2 and $(Ti,V)B_2$.

The results of this microscopy analysis based on the characterization and quantification of the microinclusions are shown in Figure 7.
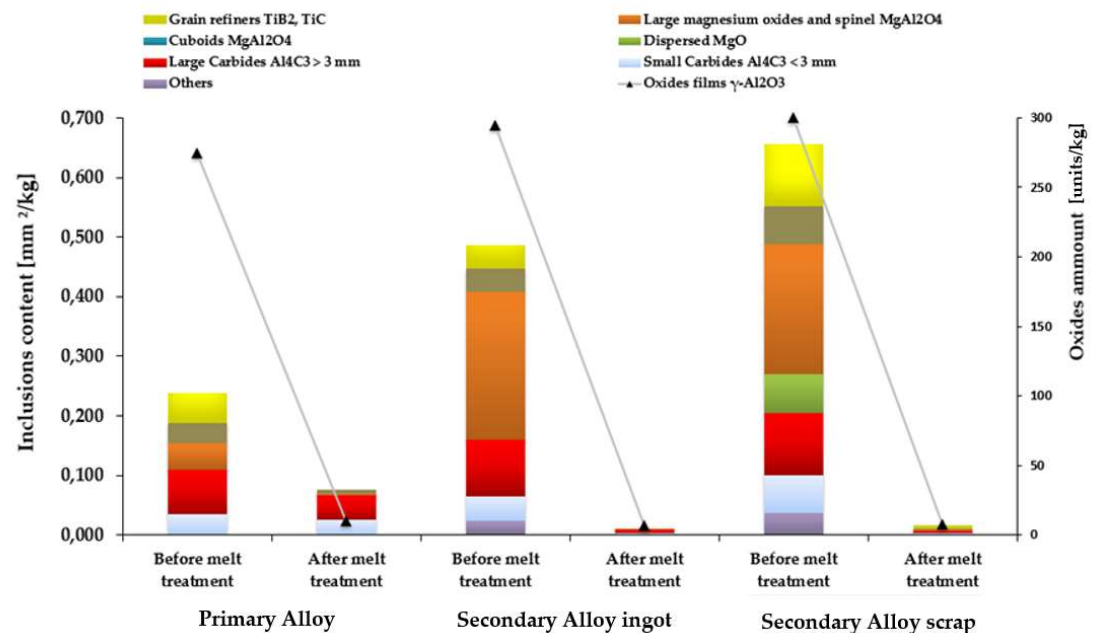

Figure 7. Quantification of each microinclusion identified in the different alloys before and after the melt treatment.

In the quantification of the inclusion is also observed that the content of microinclusions is significantly worse in the secondary alloys than in primary alloy before the melt treatment; being the secondary return alloy with a total inclusion content: $0.69 mm^2/kg$ the worst one. The difference of the inclusion content was mainly in the large magnesium oxides and spinel $MgAl_2O_4$ inclusions. Dispersed MgO are also observed in secondary

return alloy. However, the oxides film content is similar in all aluminium alloys (primary alloy has 275 oxides per kg; secondary alloy ingot: 295 per kg and finally secondary alloy return: 300 per kg). After the melt treatment, the aluminium melts improve significantly the microinclusion level in the three alloys, achieving very similar level in all of them (lower than 0.1mm²/kg microinclusions level and oxides films less than 10 per kg, and surprisingly the primary ingot has the highest value).

4. Conclusions

The melt quality of one AlSi10Mn primary alloy and of two secondary alloys obtained from different raw materials (ingot from smelter and return from two different foundries) was analysed aided by Alu Q system and microinclusion test, before and after the melt treatment. The melt treatment is based on deoxidation, degassing and skimming with detailed procedure described in this article. The main conclusion about the evolution of the melt quality before and after the melt treatment is summarized below:

- After the adding of Al90Sr10 master alloy, the eutectic temperature of the three alloys is reduced significantly, achieving similar values and a high modification rate, 4 on a 1 to 6 scale, is predicted in the three cases.

- Density Index: Before the melt treatment, the best value for the density index is achieved in the primary aluminium alloy, being significantly higher than for the rest of the alloys. However, after the melt treatment, the values of the density index are very similar in all the alloys, well below 1 %.

- The primary alloy is the cleanest in macroinclusions and microinclusions test before the melt treatment, in comparison with the two secondary alloys, being the alloy from returns the worst. However, after the melt treatment the aluminium melts improve significantly. The macroinclusion and the microinclusion levels achieve very similar values in the three alloys. The macroinclusion level is certainly very good, 9 on a 1 to 10 scale, in all alloys. In terms of microinclusion level, the melt achieves a inclusions content lower than 0.1mm²/kg and oxides films less than 10 units per kg in the three alloys.

The main conclusion is that if an adequate melt treatment is applied, it is possible to obtain recycled aluminium alloy AlSi10MnMg(Fe) with as good metal cleanliness level, density index and modification rate as primary AlSi10MnMg alloy, irrespective of the raw materials being ingots from smelter or returns.

6. Author Contributions: Conceptualization, A.B. and A.I.F.; methodology, G.P and J.L..; validation, A.N., and C.B..; formal analysis, A.N; investigation, A.B.; writing—review and editing, A.B., A.N and A.I.F.; supervision, C.B.. All authors have read and agreed to the published version of the manuscript.

Conflicts of Interest: The authors declare no conflict of interest.

References

1. Luszczak, M.; Development of High Pressure Die Casting Structural Components at Nemak Poland, 2. International Forum: Vacuum Die Casting: Structural Parts, Territet Montreux, Switzerland, March 25, Fondarex, 2015.

2. Menk W.; Automotive components in Al High Pressure Die Casting: Light weight challenge and material development, 3rd International Technical Forum on the HPDC technology, Amorebieta, Spain, November 26, 2015.

3. Rheinfeldeng Alloys GmbH & Co. KG; *Handbuch Primary aluminium casting alloys*, 2010.

4. Dobrzański L.A.; Maniara R., Sokolowski J.H.. The effect of cast Al-Si-Cu alloy solidification rate on alloy thermal characteristics. *Journal of Achievements in Materials and Manufacturing Engineering,* **2006**, *Volume 17*, pp.217-220.

5. Salas A.E.; Altamirano Guerrero R. G., Rodríguez Ortiz G., Reyes Gasga J., García Robledo J. F., Lozada Flores O., Sheilla Costa P.. Microstructural, microscratch and nanohardness mechanical characterization of secondary commercial HPDC AlSi9Cu3-type alloy. *Journal of Materials Research and Technology* **2020**, *Volume 9*, pp. 8266-8282.

6. Hu X.P.; Fang L., Zhou J.X., Zhang X.Z., Hu H.. Characterization and kinetic modeling of secondary phases in squeeze cast Al alloy A380 by DSC thermal analysis, *China Foundry*, **2017**, *Volume 14,* pp. 98-107.

7. Niklas A.; Bakedano A., Orden S., Da Silva M., Nogues E., Fernandez-Calvo A.I.. Effect of microstruture and casting defects on the mechanical properties of secondary AlSi10MnMg(Fe) test parts manufactured by vacuum assisted high pressure die casting technology, *Materials today proceedings*, **2015**, *Volume 2,*pp. 4931-4938.

8. Rheinfeldeng Alloys GmbH & Co. KG; *Handbuch Druckguss Sf-36 Ci-37 Ma-59 Ma-33*, 2007

9. Niklas A.; Bakedano A., Orden S., Da Silva M., Nogues E., Fernandez-Calvo A.I.. Microstructure and Mechanical properties of a new secondary AlSi10MnMg(Fe) alloy for ductile high pressure die casting parts for the automotive industry, *Key Engineering Material*, **2016** , *Volume 710*, pp. 244-249.

10. Gustafsson G.; Thorvaldsosson T., Dunlop G.L.. The influence of Fe, Mn and Cr on the microstructures of cast Al-Si alloys, *Metallurgical Transactions,* **1986**, *Voume 17A*, pp. 45-52.

11. Trimet Aluminium AG; *Trimal®-05 data sheet*, 2008

12. Rheinfeldeng Alloys GmbH & Co. KG. Optimizing the Mn and Mg content for structural application Silafont®-36, AlSi9MgMn, 22nd Internationational Die Casting Congress and Exposition by NADCA, Indianapolis, 2003.

13. Seifeddine S.; Svensson I. L.. The influence of Fe and Mn content and cooling rate on the microstructure and mechanical properties of A380-die casting alloys, *Metallurgical Science and Technology,* **2009**, *Volume 27 No. 1.*

14. Backerud S. L.; Chai G., Tamminen J.. Solidification Characteristics of Aluminium Alloys, *AFS*, **1990**, *Volume 2.*

15. Lu. L.; Dahle A.K.. Iron-rich intermetallic phases and their role in casting defect formation in hypoeutectic Al-Si alloys, *Metallurgical and Materials Transactions*, **2005**, *Volume 36*, pp. 819–835.

16. Gowri S., Samuel F.H.. Effect of alloying elements on the solidification characteristics and microstructure of Al-Si-Cu-Mg-Fe 380 alloy, *Metallurgical and Materials Transactions*, **1994,** *Volume 25*, pp. 437-448.

17. Samuel A.M.; Samuel F.H., Villeneuve C., Doty H.W., Valtierra S.. Effect of trace elements on β-Al5FeSi characteristics, porosity and tensile properties of Al-Si-Cu (319) cast alloys, *International Journal of Cast Metals Research*, **2001**, *Volume 14*, pp. 97-120.

18. Shabestari S.G., The effect of iron and manganese on the formation of intermetallic compounds in aluminum–silicon alloys, *Materials Science and Engineering A,***2004**, *Volume 383*, pp. 289-298.

19. Ashtari P.; Tezuka H., Sato T.. Influence of Sr and Mn Additions on Intermetallic Compound Morphologies in Al-Si-Cu-Fe Cast Alloys, *Materials Transactions*, **2003**, *Volume 44*, pp. 2611-2616.

20. Shabestari S. G.; Gruzleski J.E.. Gravity segregation of complex intermetallic compounds in liquid aluminum-silicon alloys, *AFS Trans.*, **1995**, pp. 285-293.

21. De la Fuente E.; Alfaro I., Niklas A., Anza I., Fernández-Calvo A.I.. Improved microstructure and mechanical properties of a recycled AlSi7Mg 0.3 alloy with 0.3 wt.% Fe by small additions of Mn, Cr and V, 48th Aluminium Two Thousand Congress, Milan, Italy, May 14-18, 2013.

22. Niklas A.; González-Martínez R., Orden S., Bakedano A., Garat M., Fernández-Calvo A. I.. Effect of Wall Thickness and Manganese Additions on the formation of intermetallic iron phases in new secondary alloys suitable for vacuum assisted HPDC, 121st Metalcasting Congress, Wisconsin, USA, April 25-27, 2017.

23. EP 2471967B1 granted patent. Fernández A.I., Niklas A., Alfaro Abreu I., Anza Ortiz de Apodaca I.. Method for obtaining improved mechanical properties in recycled aluminium casting free of platelet-shaped beta-phases, 2010.

24. Anantha Narayanan L., F.H. Samuel, J.E. Gruzleski J.E.. Crystallization behavior of iron-containing intermetallic compounds in 319 aluminum alloy, *Metallurgical and Materials Transactions A*, **1994,** *Volume 25*, pp. 1761-1773.

25. Hurtalova L.; Tillova E., Chalupova M.. Microstructural and Vicker Microhardness Evolution of Heat Treated Secondary Aluminium Cast Alloy, *Key Engineering Materials*, **2013**, *Volume* 586, pp. 137-140.

26. Das K.S.; Gren J.A.S.. Aluminium Industry and Climate Change-Assessment and Responses, Journal of the Minerals, Metals & Materials Society, **2010**,*Volume 62*, pp. 27-31.

27. Soo V. K.; Peeters J., Paraskevas D., Compston P., Doolan M., Duflou J. R.. Economic and Environmental Evaluation of Alu-minium Recycling based on a Belgian Case Study, 16th Global Conference on Sustainable Manufacturing, Berlin, Germany, 2018.

28. Soo V. K.; Peeters J., Paraskevas D., Compston P., Doolan M., Duflou J. R.. Sustainable aluminium recycling of end-of-life products: A joining techniques perspective, *Journal of Cleaner Production*, **2018**, *Volume 178*, pp 119-132.

29. Wetzel C S., Benchmarking Melting, *Modern Casting*, **2012**, pp. 18-21.

30. Roos H.; Optimization of the HPDC process, Technical forum Buhler, Madrid, Spain, 2016, Buhler.

31. AB B Inc; PoDFA-f system User´s Guide, Quebec, Canada, 2005.